Macromolecular Chemistry and Physics
www.mcp-journal.de

Electrical Properties of Magnetoactive Boron-Organo-Silicon Oxide Polymers

Gareth J. Monkman, Birgit Striegl, Nina Prem, and Dirk Sindersberger*

The electrical properties of rheopectic magnetoactive composites comprising boron-organo-silicon oxide dielectric matrices containing carbonyl iron microparticles are presented for the first time. The increase in interfacial magnetocapacitance is seen to greatly exceed that experienced when using conventional elastomeric matrices such as polydimethylsiloxane. In addition to the increase in capacitance, a simultaneous and sharp decrease in the parallel electrical resistance over several orders of magnitude is also observed. The effects are time dependent but repeatable. Potential applications include magnetically controlled frequency dependent devices, magnetic sensor systems, weighting elements for neural networks, etc.

1. Introduction

The mechanical and electrical characteristics of silicone elastomer-based magnetoactive polymers have been exhaustively studied over the past decade.[1] The more unusual properties of organo-silicon oxide polymers are less well known. Following research into the mechanical properties of magnetoactive boron-organo-silicon oxide polymers,[2] this work concentrates on the low frequency electrical properties of such materials and in particular interfacial magnetocapacitance and the accompanying dramatic changes in electrical resistance.

Although magnetocapacitance can exist without multiferroic coupling, magnetodielectric effects refer specifically to single-phase materials having ferroelectric and ferro- or antiferromagnetic order. Alternatives comprise composite materials combining conventional ferroelectrics and ferromagnetics segregated on a nanoscale level.[3] Intrinsic magnetodielectric coupling must be separated from interfacial magnetocapacitance.[4] Consequently, the magnetodielectric effect implies electromagnetic coupling at the atomic, or at least molecular, level where the relative permittivity of the dielectric may change when subjected to a magnetic field. At the other end of the mesoscopic scale, where micrometer sized particles are distributed within a polymer dielectric matrix, changes in capacitance are due purely to rearrangements in the magnetic particle structure while the relative permittivity of the dielectric matrix always remains uninfluenced. This can be seen from capacitance calculation used in the analysis and simulation of magnetoactive polymers.[5]

In order to avoid confusion, the term "interfacial magnetocapacitance" will be adopted throughout this paper. The related effects on electrical resistance experienced by boron-organo-silicon oxide magnetoactive materials through the application of an external magnetic field will also be discussed.

The often used term "dielectric constant" is incorrect in that ε_r is a function of frequency and temperature (i.e., not a constant in the strict meaning of the term). The correct name for ε_r is relative permittivity and the absolute permittivity ε is the product of free space permittivity ε_0 and relative permittivity ε_r.[6] For clarity, this (correct) nomenclature will be adopted throughout this paper.

2. Magnetoactive Polymers

Magnetoactive polymers (MAP) are elastomeric composites comprising a nonmagnetic polymer matrix and a distribution of magnetically susceptible micrometer sized ferromagnetic or paramagnetic particles.[7] They undergo a distinct increase in Young's modulus with the application of an external magnetic field.[8] When subjected to inhomogeneous magnetic fields, magnetodeformation may be experienced making them suitable for the development of small actuators and even complete devices.[9] Though the main contribution to actuation lies in magnetodeformation in a nonlinear magnetic field, slight magnetostriction has also been observed in homogeneous magnetic fields.[10]

The most common matrix materials used for MAP fabrication are silicones, particularly polydimethylsiloxane (PDMS), though occasionally polyurethane has also been used.[11] Carbonyl iron powder (CIP) is the most commonly used soft magnetic filler material, though hard magnetic materials such as NdFeB have also been employed.[12] Due to conventional fabrication techniques, the magnetic particle distributions can be isotropic or anisotropic though perfect dispersion homogeneity is difficult to achieve. In addition to their basic mechanical

Prof. G. J. Monkman, Dr. N. Prem, Dr. D. Sindersberger
Mechatronics Research Unit
OTH
Regensburg 93053, Germany
E-mail: gareth.monkman@oth-regensburg.de
Dr. B. Striegl
Centre for Biomedical Engineering
OTH
Regensburg 93053, Germany

The ORCID identification number(s) for the author(s) of this article can be found under https://doi.org/10.1002/macp.201900342.

DOI: 10.1002/macp.201900342

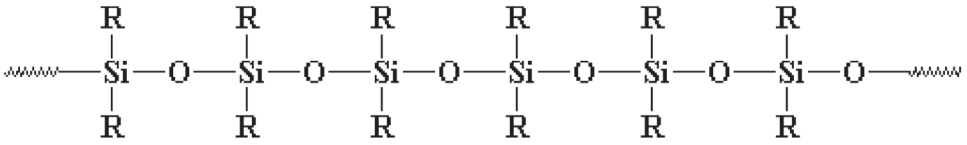

Figure 1. Polyorganosiloxane polymers, commonly called silicones.

properties, magnetoactive polymers exhibit interesting electrical properties. Interfacial magnetocapacitance often quoted as "magnetodielectric effect" (sic), complex impedance, etc. have all been evaluated for different magnetic content under various ranges of applied magnetic field.[13–15] However, a magnetoactive elastomer with a CIP concentration of 73%, subject to an applied magnetic field strength of 700 000 A m^{-1}, exhibits little more than a 60% increase in capacitance.[16]

Where the particles are not constrained by an elastic matrix but allowed to migrate in a viscoelastic medium, dramatic effects on the electrical capacitance and resistance become clearly observable. The remainder of this work deals exclusively with such interfacial magnetocapacitive effects in boron-organo-silicon oxide polymers.

3. Boron-Organo-Silicon Oxide Polymers

Certain organo-silicon oxide polymers demonstrate viscoelastic-plastic characteristics such as rheopexy. The combination of dimethylsiloxane and boric acid dates back to two patents filed during the 1940s.[17,18] The original compound comprised 65% dimethylsiloxane (hydroxy-terminated polymers with boric acid), 17% silica (crystalline quartz), 9% Thixotrol ST (castor oil derivative), 4% polydimethylsiloxane, 1% decamethyl cyclopentasiloxane, 1% glycerine, and 1% titanium dioxide,[19] and the majority of modern compounds deviate little from this. The material is even marketed as a toy under the name "Silly Putty." Industrial uses include deburring and polishing.

Silicones consist of polymeric chains with an alternating silicon–oxygen backbone having various organic groups bonded to each silicon atom, as shown in **Figure 1**. In the case of PDMS, the organic section comprises methyl groups.

Fluids, emulsions, lubricants, resins, elastomers, or rubbers are different classes of commercially important silicone products. The elastic behavior of polymers is based on the wide-meshed cross-linking of the molecular chains. Cross-linking prevents the polymer chains from sliding apart, as is the case with liquids. The re-deformation after elongation of an elastomer is based on changes in entropy.

Silicone rubbers without filler materials demonstrate low viscoelasticity. The cross-linking of the polymer chains inhibits viscous yielding. Usually, the rubbery-elastic properties of silicone elastomers without reinforcement dominate. The addition of even small amount of nanoparticle fillers such as silica powder is able to change the viscoelastic properties of silicone rubbers significantly.[20] The substitution of between 1% and 30% silicon atoms (Si) of the polymer chain by boron atoms results in a boron-silicone material with definite viscoelastic properties. This viscoelastic effect is based on the temporary bonding between an oxygen electron pair and the boron atom.

Many solid silicone compounds demonstrate little change in elastic modulus between −150 °C and the glass transition at around 200 °C after which they become much softer.[21] With organo-silicon oxide polymers, reduced viscosity commences abruptly at around 60 °C.[22] In this work, all investigations have been carried out at temperatures well under 60 °C.

4. Magnetoactive Boron-Organo-Silicon Oxide Polymers

The combination of carbonyl iron particles with boron-organo-silicon oxide polymers does not result in an elastomer as with traditional PDMS materials because boron-organo-silicon oxide polymers are viscoelastic. Low strain rate deformation is inherently plastic rather than elastic. In the case of a PDMS-based MAP, the magnetic field induced displacement of a magnetic particle is always limited by the elasticity of the polymer matrix in which the particles are held.

$$\sigma = k\gamma^n \tag{1}$$

The tangential stress σ of a dilatant (shear thickening) fluid is given by (1) where k is a constant and the shear rate γ is raised to some power n in accordance with the Ostwald-de Waele model. For a rheopectic material such as boron-organo-silicon, $n > 1$.[23]

5. Experimental Section

Commercially available boron-organo-silicon oxide polymers (www.knete.de) were combined by mechanically kneading carbonyl iron powder (CIP) particles with diameter range 3.9–5 µm (BASF SQ) at a temperature of 37 °C. Samples containing between 5% and 60% CIP were fabricated. Higher concentrations were difficult to achieve as particulate absorption approached saturation resulting in increasing inhomogeneity.

The distance between the electrodes was maintained by a 1 mm wide electrically insulating ring as shown in the exploded sample illustration in **Figure 2**. The capacitive effects of the plastic ring were found to be insignificant and so could be neglected.

In order to rule out any equipment idiosyncrasies, two forms of magnetic field generation were employed. The first, as shown in Figure 2, employed permanent magnets where the distance between the poles is adjustable. The adjustable iron yoke also serves to complete the magnetic circuit between the permanent magnets. The second method utilized two coils of 1440 turns on a closed common soft iron former driven from two stabilized high-current power supplies (Sorensen DCR 60-45B). Samples were inserted mechanically using a Stäubli RX60 [24]

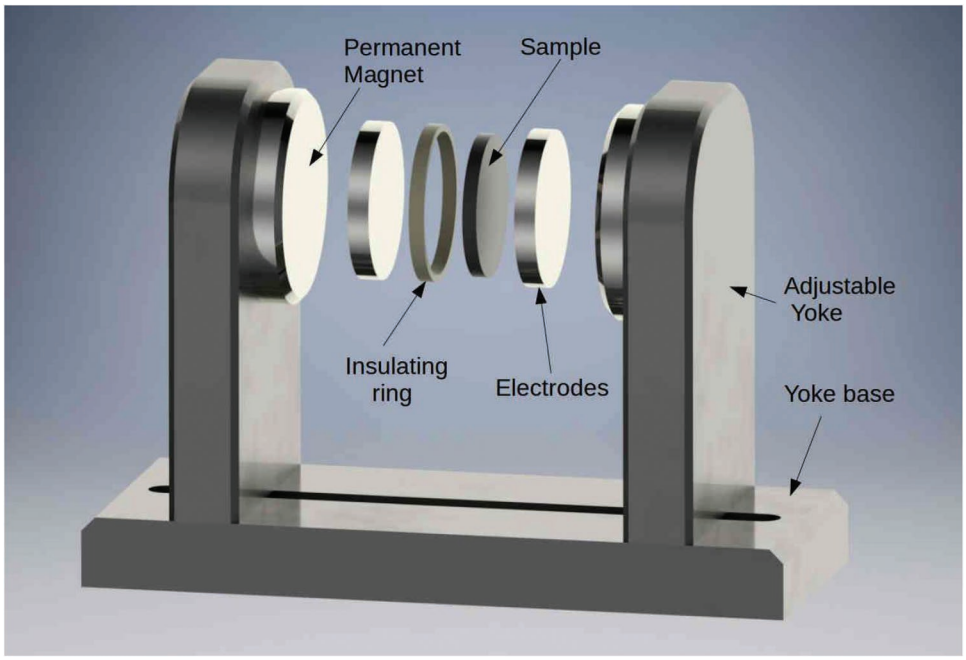

Figure 2. Permanent magnet field generation (with exploded view of sample and electrodes).

robot within 50 ms. Measurements of magnetic flux density within the yoke gap were made using a gaussmeter (LakeShore 455 DSP) placed in the center of the sample by means of a small aperture in the insulating ring. In the interests of clarity, the wiring and sensor devices are not shown in **Figures** 2 and **3**.

As the distance between the solenoid poles remained constant, no significant changes to the magnetic field homogeneity were observed. However, with the permanent magnet apparatus, the magnetic field could only be varied according to the distance between the poles. This was found to agree well with the magnetic field generated by the solenoids for flux densities between 200 and 350 mT.

Initially, samples without CIP were placed between, and in contact with, the two 38 mm diameter aluminum electrodes. Electrical measurements were made on samples of thickness (d in (2)) 1.0, 1.6, 2.2, and 3.0 mm. The capacitance of the boron-organo-silicon oxide polymer alone was measured using the apparatus described above. Rearranging the usual planar

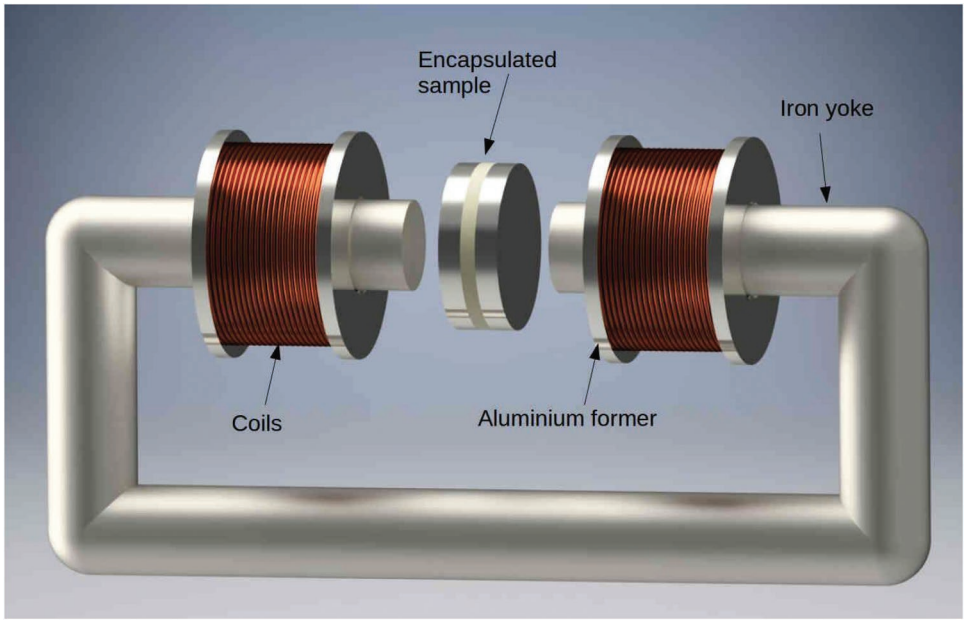

Figure 3. Inductive field generation (with collapsed view of sample and electrodes).

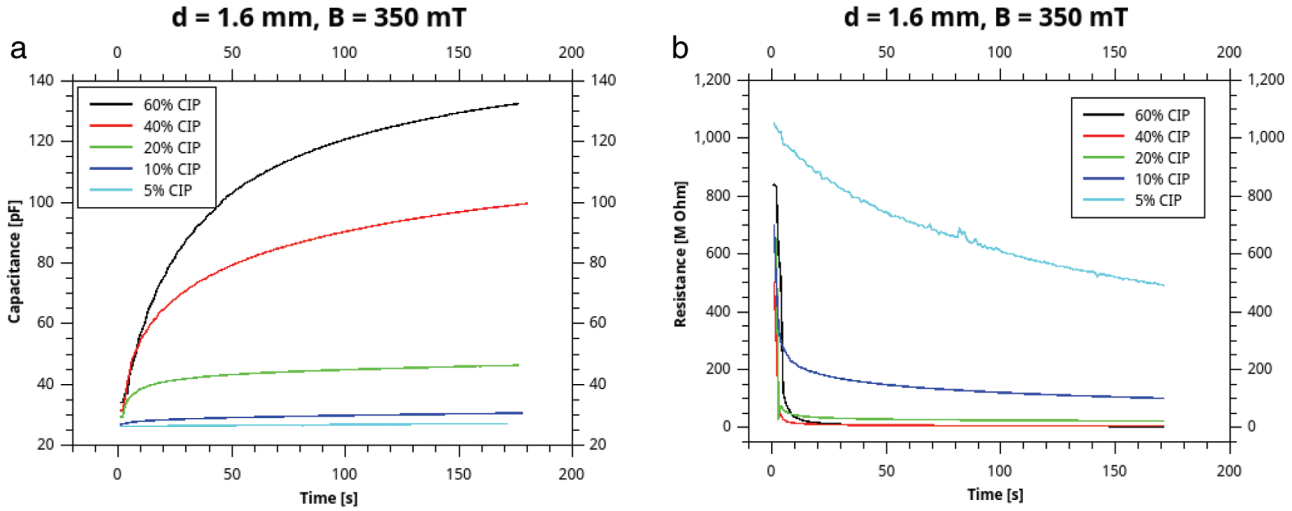

Figure 4. For various CIP concentrations, a) capacitance versus time, b) resistance versus time.

capacitance expression (2) for ε_r revealed a relative permittivity of 3.7 for all three sample thicknesses.

$$C = \frac{\varepsilon_0 \varepsilon_r A}{d} \tag{2}$$

Although as mentioned previously, relative permittivity is not a constant but has a degree of frequency dependence, the ε_r of boron-organo-silicon oxide polymers remains relatively stable from 100 Hz to 50 kHz before slowly rising to around 4 as the frequency is increased to 100 kHz. Above this frequency, the influence of stray capacitance was found to introduce inaccuracies. Regardless of frequency, the raw material measurements were uninfluenced by the applied magnetic field. The remainder of the measurements using magnetoactive boron-organo-silicon oxide compounds were carried out at a frequency of 1 kHz.

Samples containing 5%, 10%, 20%, 25%, 40%, and 60% CIP by mass were produced and tested using the apparatus mentioned above in the same way as those without magnetic content.

The electrical properties, namely capacitance and resistance were measured simultaneously using a programmable LCR bridge (Hameg HM8118) connected to a computer by means of the instruments RS232 interface. The software interface (ZOC) was programmed using REXX script and data collected at various acquisition rates. As the initial resistance was in excess of what the LCR bridge could measure, the initial 20 mS of data have not been included. Due to the dramatic, and unexpected, changes in capacitance and resistance, the experiments were verified using a Philips PM6303 RCL Meter.

6. Measurement Results

As seen in **Figure 4**, the capacitance and resistance change significantly with CIP content. At 60% CIP, a threefold increase in capacitance is observable whereas with only 5% CIP content the effect is considerably weaker. The initial capacitance without CIP can be calculated from formula (2) as ≈23 pF. The addition of CIP increases this quiescent capacitance to around 40 pF. On the application of a magnetic field with flux density 350 mT, the capacitance rises exponentially as shown in Figure 4a. At the same time the resistance sinks even more dramatically as shown in Figure 4b). The initial values of resistance prior to the application of a magnetic field were often beyond the scale of the instrument (in the GΩ range) and for clarity and graphical scaling purposes, the first few measurements have been omitted. The resulting effects correlate well with the CIP content.

On the other hand, the relaxation curves shown in **Figure 5** demonstrate a more rapid return to the original conditions on removal of the magnetic field.

Discernible between Figures 4 and 5 is also a very large degree of hysteresis. This is due to the fact that the final physical relaxation of the compound occurs over several hours. This long relaxation time may appear as a disadvantage at first sight. However, where shape memory effects are concerned, this phenomenon is of major interest.[25]

Figures 6 and **7** show the relationships between capacitance and resistance after 180 s for different percentages of CIP content.

Most interesting are the effects of increasing magnetic flux density. Figure 6 shows the increase in capacitance for the: a) 20% CIP, b) 40% CIP, and c) 60% CIP samples with magnetic flux densities of 250, 300, and 350 mT, respectively. Here, it can be observed that the increase in capacitance is predominantly a function of the CIP concentration. In fact, the magnetic flux density influences only the time constants, which are at least 15, 18, and 35 s, respectively. As pointed out earlier, the final steady state will only be reached after several hours and so these values serve only as a guide for the measurement duration of 180 s.

Conventional MAP demonstrate a similar, though far less dramatic reduction in electrical resistance for an applied magnetic field.[26] Although the magnetic reaction for magnetorheological fluids takes place within 20 ms, the mechanical reaction can be twice this.[27] Magnetoactive polymers are magnetoelastic so the change can take up to several seconds.[15] Furthermore, organo-silicon oxide materials are rheopectic so

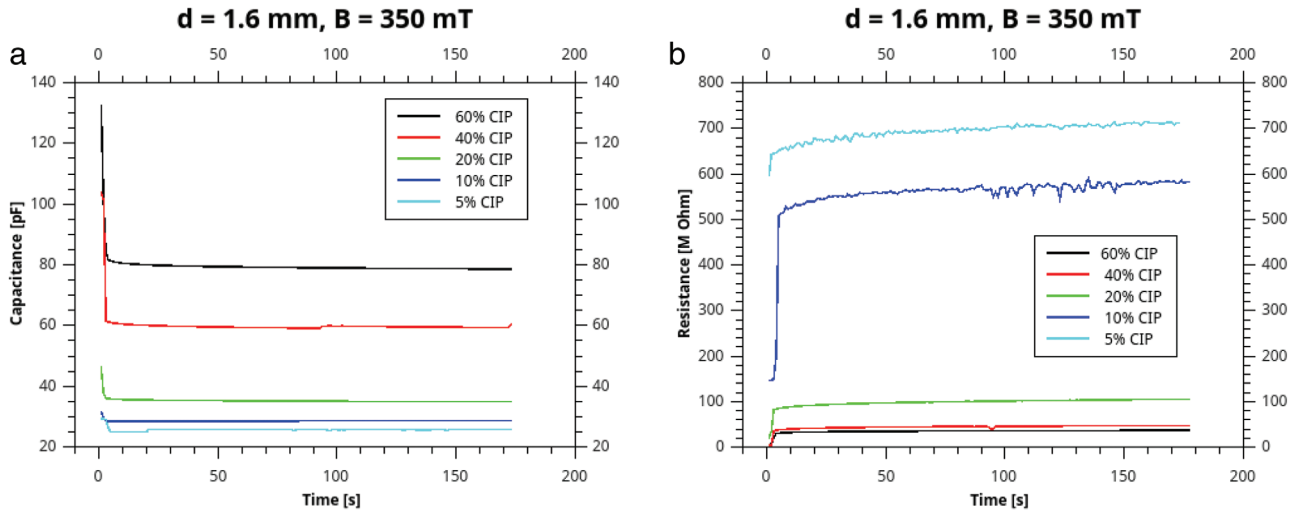

Figure 5. For various CIP concentrations, a) capacitance versus decay time, b) resistance versus rise time.

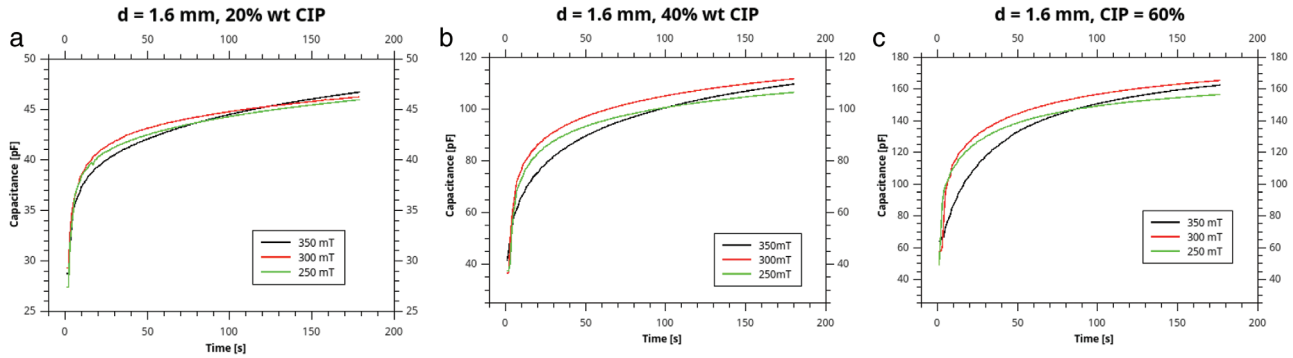

Figure 6. Capacitance rise time for a) 20% CIP, b) 40% CIP, and c) 60% CIP.

the matrix resists rapid CIP displacement but allows slow creep and relaxation.

This latter is almost certainly due to the rheopectic properties of boron-organo-silicon oxide resulting in a slower response at high magnetic flux densities. Although the steady-state capacitance values shown in Figure 6 follow an exponential rise time curve, the resistance graphs of Figure 7 show an abrupt decrease from the quiescent state of an effective insulator to a resistance of only a few MΩ.

7. Analysis

Without magnetic content, the relationship between capacitance and gap width d follows exactly that of expression (2). However, when CIP is present, less dielectric volume is available and the increase in capacitance as a result of gap width reduction is consequently limited. This can be seen in **Figure 8** where the capacitance merely doubles whereas according to (2) it would normally be three times higher for a reduction of d from 3 to 1 mm.

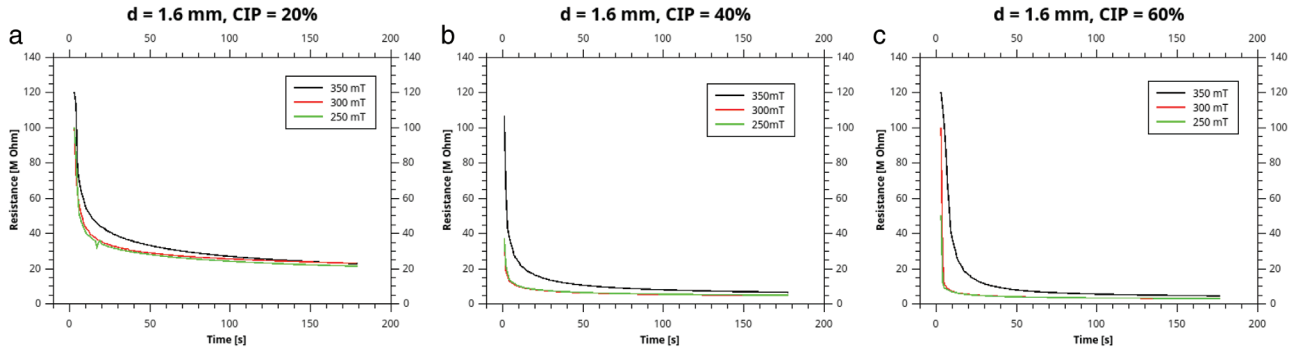

Figure 7. Resistance decay time for a) 20% CIP, b) 40% CIP, and c) 60% CIP.

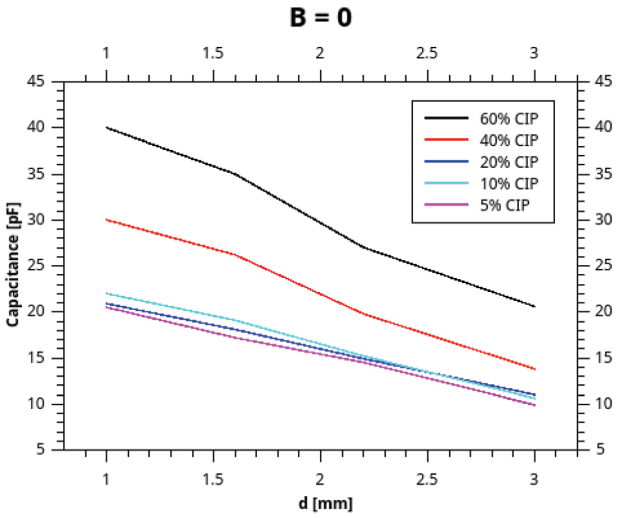

Figure 8. Capacitance without magnetic field for different gap widths.

This cannot be attributed alone to the fact that the volume fraction of dielectric reduces with increasing CIP mass fraction. The volume fraction of dielectric reduces with increasing CIP mass fraction. The density of iron ρFe is 7860 kg m^{-3} whereas that of boron-organo-silicon oxide polymer ρp is just over 1000 kg m^{-3}. Consequently, a 60% CIP mass fraction equates to a mere 16% CIP volume fraction.

Given that both A and ε_r in (2) remain the same, for a given CIP content only d changes. Consequently, any change in C must be directly proportional to a change in d. However, the change in d is not simply the distance between two electrodes. The intrinsic electrodes, in this case are the CIP particles themselves. Assuming spherical particles, in the absence of a magnetic field, the particles are arranged randomly as in **Figure 9**a,c. On the application of a magnetic field, they become aligned as in Figure 9b,d.

A volume fraction is simply the mass fraction M divided by the ratio of the two material densities. For a symmetrical cube, the square of the cube root of a given volume provides the effective area of CIP content visible on one face of a symmetrical cube (3).

$$A = \left(\frac{M\rho_p}{\rho_{Fe}} \right)^{2/3} \tag{3}$$

Calculating the areas according to (3) allows the simple model of Figure 9 to be drawn to scale in order to show a more realistic picture. The sum of the areas of the particles shown corresponds to respective areas as a function of the frame around them, that is, A = 5.4% for 10 wt% CIP and A = 18% for a 60 wt% CIP.

With such a high CIP concentration, a more complex agglomeration is very likely with particle pairing or clustering making the simplified model of Figure 9 less accurate.

Figure 10 shows X-ray tomography images taken using a micro-CT system (GE Phönix v|tome|xs 240/180) at 65 kV, 195 µA, voxel size 3 µm. The boron-organo-silicon oxide sample containing 5 wt% CIP is constrained within a glass vial. This lower percentage of filler was necessary as higher percentages became opaque to the X-ray radiation.

The color bars to the left indicate the concentration in mm^3. Figure 10a shows the sample in its initial state directly after mixing without magnetic field. Although movement of the CIP commences immediately on applying a magnetic field, full alignment of the particles takes some time. Figure 10b shows the situation after several days subjected to a magnetic field applied immediately below the sample (providing a magnetic flux density of 390 mT at the sample base, reducing to 120 mT at the top).

As can be seen from Figure 10a, the dispersion after mixing still contains a few clusters (orange color) but is otherwise without any clear structure. Following the application of a magnetic field, very clear orientation and alignment of the particles can be seen. At higher CIP percentages, the samples were too dense to produce reliable X-ray images.

8. Discussion

The drastic reduction in electrical resistance can be attributed to alignment of the CIP within the polymer matrix. Due to the inherent elasticity of conventional PDMS-based MAP, only partial particle alignment is possible and particle contiguation is very limited. In a boron-organo-silicon compound, as the particles move to align themselves with the magnetic field, a degree of interparticle contact becomes more likely. This has a limited effect on the capacitance but inevitably serves to increase the electrical conductivity. There are various theories to these ends including the jamming[28] and percolation theories relevant to both magnetorheological fluids[29] and polymer composites.[30] The jamming theory has also been investigated specifically for

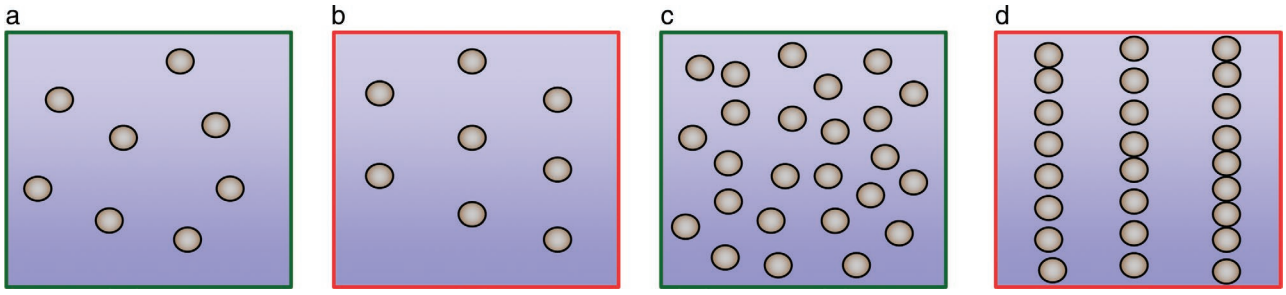

Figure 9. a) 10 wt% CIP random, b) 10 wt% CIP aligned, c) 60% CIP random, d) 60% CIP aligned.

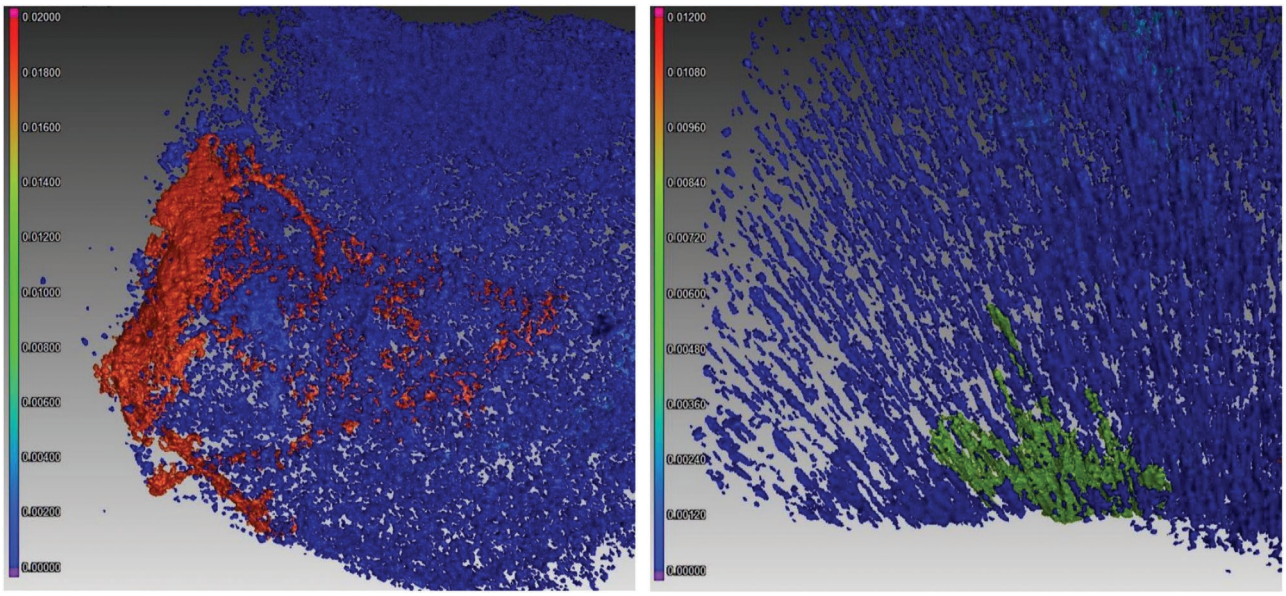

Figure 10. X-ray tomography image of 5 wt% CIP boron-organo-silicon oxide polymer.

shear thickening organo-silicon oxide polymers.[31] However, before the reader embarks upon an analysis of exotic theories, a closer look at the situation may reveal more.

Figure 4b illustrates the situation well. At high CIP mass fractions (>20%), the effect reaches a saturation level regardless of the magnetic flux density as shown in Figure 7. At lower CIP mass fractions, the drop in electrical resistance follows a more traditional decay curve proportional to the reciprocal of the interparticle distance. However, due to the magnetic field, this distance is constantly reducing which further expedites the drop in electrical resistance.

As seen in all the curves, there are clearly two different time constants involved. The first is extremely short and represents the immediate reaction to the magnetic field as the particles separate from one another thus destroying cluster formations. The second time constant is much longer and results from the slow orientation of the particles into chains which is considerably slower due to the viscoelastic properties of the matrix material as illustrated in Figure 9.

9. Applications

The ability to magnetically control electrical capacitance and resistance has many potential applications in the electronics industry. This is particularly relevant to magnetic switching in high voltage applications where initially a high breakdown resistance is important.[32] The use of magnetoactive polymers against piezoresistive membranes in order to control high voltages intended for the driving of dielectric actuators has been proposed.[33] The use of boron-organo-silicon-based devices would simplify this considerably.

Related to applications concerning the measurement of magnetic fields, memristors and memcapacitors for use in neural networks are an emerging technology which demands the ability to weight individual node inputs by means of externally controllable resistance, capacitance, or inductance.[34] Boron-organo-silicon fulfills the first two criteria. The third, inductance, remains to be investigated.

10. Conclusions

This work has demonstrated how interfacial magneto-capacitance in magnetoactive boron-organo-silicon oxide polymers may be significantly influenced by applied magnetic fields having flux densities under 350 mT. A considerable increase in electrical capacitance compared to that found with conventional PDMS-based magnetoactive polymers has been observed. Simultaneously, an abrupt reduction in parallel electrical resistance of several orders of magnitude is experienced. Both these properties are attributed to particle contiguation during the magnetic field induced alignment process. This latter has been confirmed by a series of X-ray tomography measurements.

Acknowledgements

The authors would like to express their thanks to the Deutsche Forschungsgemeinschaft (DFG) for financial support within the SPP1681 (MO 2196/2-1) research program and in the acquisition of X-ray tomographic equipment for research (INST 102/11 – 1 FUGG).

Conflict of Interest

The authors declare no conflict of interest.

Keywords

boron-organo-silicon oxide, interfacial magnetocapacitance, magnetoactive, polymer

Received: August 9, 2019
Revised: November 10, 2019
Published online: January 15, 2020

[1] P. Melenev, Y. L. Raikher, V. V. Rusakov, *Polym. Sci. A* **2010**, *52*, 430.
[2] F. Guo, C.-B. Du, R.-P. Li, *Adv. Mech. Eng.* **2014**.
[3] G. Catalan, *Appl. Phys. Lett.* **2006**, *88*, 102902.
[4] G. Lawes, G. T. Kimura, C. M. Varma, M. A. Subramanian, N. Rogado, R. J. Cava, A. P. Ramirez, *Prog. Solid State Chem.* **2009**, *37*, 40.
[5] D. Isaev, A. Semisalova, Y. Alekhina, L. Makarova, N. Perov, *Int. J. Mol. Sci.* **2019**, *20*, 1457.
[6] IEEE 211-1997—IEEE standard definitions of terms for radio wave propagation, https://doi.org/10.1109/IEEESTD.1998.87897 (accessed: December 2019).
[7] R. Ahamed, M. M. Ferdaus, *J. Intell. Mater. Syst. Struct.* **2018**, *29*, 2051.
[8] A. Stoll, M. Mayer, G. J. Monkman, M. Shamonin, *J. Appl. Polym. Sci.* **2014**, *131*, app.39793.
[9] K. Zimmermann, V. Böhm, T. I. Becker, J. Chavez Vega, T. Kaufhold, G. J. Monkman, D. Sindersberger, A. Diermeier, N. Prem, *Prob. Mech.* **2017**, *4*, 5.
[10] V. Sorokin, G. Stepanov, M. Shamonin, G. J. Monkman, A. R. Khokhlov, E. Y. Kramarenko, *Polymer* **2015**, *76*, 191.
[11] K. Petcharoen, A. Sirivat, *Mater. Sci. Eng., C* **2016**, *61*, 312.
[12] H. Böse, A. Hesler, G. Monkman, *Deutsche Patent DE 10 2007 028 663 A1*, 2011.
[13] I. Bica, *J. Ind. Eng. Chem.* **2012**, *18*, 1666.
[14] I. Bica, Y. D. Liu, H. J. Choi, *Colloid Polym. Sci.* **2012**, *290*, 1115.
[15] I. A. Belyaeva, E. Y. Kramarenko, M. Shamonin, *Polymer* **2017**, *127*, 119.
[16] A. S. Semisalova, N. S. Perov, G. V. Stepanov, E. Y. Kramarenko, A. R. Khokhlova, *Soft Matter* **2013**, *9*, 11318.
[17] R. R. McGregor, E. L. Warrick, *US Patent No. 2,431,878*, **1947**.
[18] J. G. E. Wright, *US Patent No. 2,541,851*, **1951**.
[19] T. Ikematu, Y. Kishimoto, K. Miyamoto, *US Patent No. 5,189,110*, **1993**.
[20] KulikV. M. , A. V. Boiko, S. P. Bardakhanov, H. Park, H. H. Chun, I. Lee, *Mater. Sci. Eng., A*, **2011**, *528*, 5729.
[21] C. Hamciuc, E. Hamciuc, L. Okrasa, *Macromol. Res.* **2011**, *19*, 250.
[22] M. P. Goertz, X.-Y. Zhu, J. E. Houston, *J. Polym. Sci., Part B: Polym. Phys.* **2009**, *47*, 1285.
[23] J. Ferguson, Z. Kemblowski, *Applied Fluid Rheology*, Elsevier, London **1991**.
[24] Stäubli, RX60 Robot, CS7M controller – D.280.059.04.F – 11/1999.
[25] G. J. Monkman, *Mechatronics* **2000**, *10*, 489.
[26] I. Bica, E. M. Anitas, M. Bunoiu, B. Vatzulik, J. Juganaru, *J. Ind. Eng. Chem.* **2014**, *20*, 3994.
[27] H. Sahin, F. Gordaninejad, X. Wang, Y. Liu, *J. Intell. Mater. Syst. Struct.* **2012**, *23*, 949.
[28] V. Trappe, V. Prasad, L. Cipelletti, P. N. Segre, D. A. Weitz, *Nature* **2001**, *411*, 772.
[29] D. T. Zimmerman, R. C. Bell, J. A. Filer, J. O. Karli, N. M. Wereley, *Appl. Phys. Lett.* **2009**, *95*, 014102.
[30] A. J. Marsden, D. G. Papageorgiou, C. Vallés, A. Liscio, V. Palermo, M. A. Bissett, R. J. Young, I. A. Kinloch, *2D Mater.* **2018**, *5*, 032003.
[31] S. Gürgen, W. Li, M. C. Kuşhan, *Mater. Des.* **2016**, *104*, 312.
[32] O. Zappa, G. J. Monkman, S. Egersdörfer, G. Datzer, W. Kahled, H. Böse, A. Tunayer, presented at Actuator 2004, Bremen, Germany, June **2004**.
[33] M. Henke, G. Gerlach, *J. Intell. Mater. Syst. Struct.* **2016**, *27*, 375.
[34] F. Caravelli, J. P. Carbajal, *Technologies* **2018**, *6*, 118.